Jie Ma
Key Laboratory of Soft Machines and Smart Devices of Zhejiang Province,
X-Mechanics Center,
Department of Engineering Mechanics,
Zhejiang University,
Hangzhou 310027, China
e-mail: 11824009@zju.edu.cn

Zheng Jia[1]
Key Laboratory of Soft Machines and Smart Devices of Zhejiang Province,
X-Mechanics Center,
Department of Engineering Mechanics,
Zhejiang University,
Hangzhou 310027, China
e-mail: zheng.jia@zju.edu.cn

Shaoxing Qu
Key Laboratory of Soft Machines and Smart Devices of Zhejiang Province,
X-Mechanics Center,
Department of Engineering Mechanics,
Zhejiang University,
Hangzhou 310027, China
e-mail: squ@zju.edu.cn

A Constitutive Model for Binary-Solvent Gels

A hydrogel is a network of polymeric chains hosting a large amount of the single solvent, namely, water. The high degree of hydration not only endows hydrogels with desired attributes such as superb biocompatibility but it also yields disadvantages, including high volatility and inability to host hydrophobic drugs. The need for enhancing the versatility of hydrogels to meet requirements of diverse applications has led to the fabrication of binary-solvent gels (e.g., gels in aqueous ethanol) with the hope to capitalize on both the merits of water and other organic solvents. In this paper, to understand the fundamental mechanics of binary-solvent gels, we develop a constitutive model by formulating the free energy function based on the extended Flory–Huggins lattice theory and deriving the equilibrium equations. We then apply the model to examine the mechanical behaviors of binary-solvent gels under mechanical forces, or subject to geometric constraints. The model can consistently capture some experimental findings on binary-solvent gels such as the cononsolvency effect. In particular, we employ the model to analyze a bilayer soft actuator consisting of a binary-solvent gel film attaching to a passive polymer substrate. The proposed model may provide insights into the design of novel soft machines based on binary-solvent gels. [DOI: 10.1115/1.4047116]

Keywords: constitutive model, binary-solvent gels, free energy function, constraints, soft actuator, elasticity, stress analysis

1 Introduction

Hydrogels are three-dimensional networks of hydrophilic polymeric chains that host a large amount of water, from a few percent to thousands of times of their dry weight. The crosslinked long-chain polymer network makes hydrogel solid-like and highly deformable, and the high degree of hydration provides physical similarity to tissues and endows hydrogels with excellent biocompatibility. Owing to the aforementioned merits, hydrogels are attractive for many applications in diverse technologies, including tissue engineering [1,2], drug delivery [3–5], bioelectronics [6,7], and energy storage [8]. Despite the success of hydrogels in a broad range of applications, the water-rich polymeric aggregates still face problems that originate from the high concentration of water. For example, due to the volatile nature of water, most hydrogels severely suffer from poor long-term stability since they dry out very fast in open environments [9]. Moreover, although hydrogels provide ideal platforms for controlled drug delivery, many drugs and nutrients have poor solubility in water so that hydrogel carriers can hardly deliver them [4,10]. To address these shortcomings attributed to water, which is the single solvent in hydrogels, binary-solvent gels have been developed, which bring together the inherent merits of hydrogels with the attributes of other organic solvents such as hydrophobicity and non-volatility. Examples include but are not limited to novel drug delivery systems based on binary-solvent gels which can carry both hydrophilic and hydrophobic drugs [11], and gels formed in a binary solvent with enhanced capacity of water retention [12].

The emergence of a myriad of functional hydrogels and their broad applications has motivated recent developments of the constitutive models for hydrogels. A nonlinear field theory of the hydrogel was formulated by extending the Flory–Rehner function, accounting for both the stretching of the polymer network and the mixing of polymer chains and water molecules [13]. In addition, a number of theoretical frameworks have been put forward to unravel the underlying mechanisms of hydrogels deforming in response to different stimuli, including the variation of temperature [14], salinity [15], pH [16], and light [17,18]. Mechanical behaviors such as contact [19], damage [20,21], phase transition [22], viscoelasticity [23], instability [24–26], self-healing [27,28], and anisotropicity [29] have also been taken into account by mechanistic models for hydrogels. Extensive efforts have been devoted to the mechanics of hydrogels, namely, a gel in a single solvent of water. In contrast, very few models have been developed to represent mechanical responses of binary-solvent gels, with two types of solvent molecules mixing with the polymer chains (Fig. 1). The swelling of polydimethylsiloxane (PDMS) membranes in the mixture of water and ethanol was studied by adopting the Flory–Huggins model [30]. By resorting to the statistical association fluid theory, the degree of swelling and the gel-phase composition

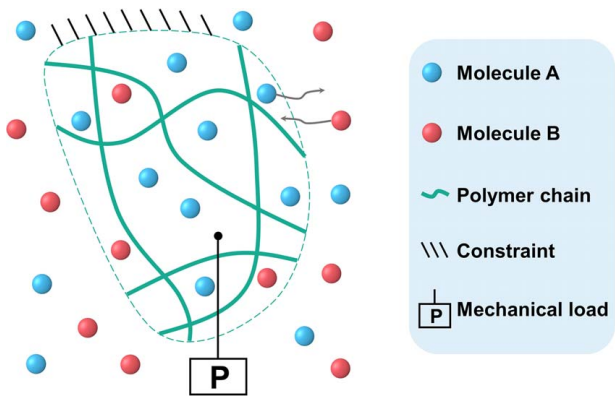

Fig. 1 A binary-solvent gel is in contact with an external binary solvent of two different types of molecules (namely, A and B) and is subject to mechanical loads and geometric constraints. The gel exchanges solvent molecules with the external solvent to attain equilibrium of the system.

[1]Corresponding author.

Contributed by the Applied Mechanics Division of ASME for publication in the Journal of Applied Mechanics. Manuscript received March 16, 2020; final manuscript received April 28, 2020; published online May 29, 2020. Assoc. Editor: Yonggang Huang.

of poly(N-isopropylacrylamide) gels in water and alcohols were investigated [31]. A thermodynamic framework was reported to explain the cosolvency and cononsolvency effects of gels swelling in the binary solvent [32]. These studies focused on the free swelling of gels in the binary solvent in the absence of mechanical constraints and forces, such that the understanding of mechanical behaviors of binary-solvent gels in response to applied loadings remains opaque. Notably, mechanical responses of gels in response to even simple loadings can be of practical significance. For instance, it has been demonstrated that hydrogels absorb water and expand in volume when being stretched, and such swelling behavior in response to tension may result in a novel instability mode, the delayed instability [24]. However, it remains unclear whether gels in binary solvents swell or shrink when subject to tensile stresses. To this end, a constitutive framework that can be applied to study the intricate interplays among applied stresses, deformation of gels, and external solvents is highly desired.

In this article, we outline a simple yet generic constitutive model to investigate the mechanical response of a gel in equilibrium with binary solvent and mechanical forces. In Sec. 2, we present the fundamental assumptions and formulations of the model. The free energy due to mixing polymer chains with two types of solvent molecules is derived by linking an extended Flory–Huggins lattice theory to the framework of continuum mechanics. The equations of state are presented in the most generic form. In Sec. 3, we apply the constitutive model to binary-solvent gels subject to different types of mechanical forces or constraints, as many applications require gels to deform under external forces or constraints. In particular, we analyze a bilayer soft actuator consisting of a binary-solvent gel film attaching to a passive polymer substrate. Concluding remarks are given in Sec. 4.

2 Formulation of the Model

We aim at developing a thermodynamic-based model for binary-solvent gels. As sketched in Fig. 1, the binary-solvent gel is conceptualized as an aggregate of a network of crosslinked polymer chains and two types of solvent molecules (namely, solvents A and B), which is in contact with an external binary solvent and subject to a set of mechanical forces and geometrical constraints. For this system, we will first formulate the free energy function for binary-solvent gels, and then implement the free energy function to the thermodynamic framework to derive the equilibrium equations.

2.1 The Free Energy Function. Since the hydrogel is an aggregate of a network of crosslinked polymer chains and two types of solvent molecules, the free energy density W can be postulated as a summation of the strain energy density W_{stretch} associated with the stretching of the network and the contribution W_{mix} due to the mixing of the network and the binary solvent; that is

$$W = W_{\text{stretch}} + W_{\text{mix}} \tag{1}$$

For polymer chains crosslinked into a three-dimensional network, the free energy density due to the stretching of the network is taken to be

$$W_{\text{stretch}} = \frac{1}{2} NkT[F_{ik}F_{ik} - 3 - 2\log(\det \mathbf{F})] \tag{2}$$

where N is the nominal density of the polymer chains, i.e., the number of polymer chains divided by the volume of the dry polymer. $\mathbf{F}$ is the deformation gradient of the network, and $F_{iK}F_{iK}$ and $\det \mathbf{F}$ are invariants of the deformation gradient.

We next formulate the unspecified free energy density W_{mix} arising from mixing polymer chains and two types of solvent molecules. In many gels, the density of the crosslinks is very low since each polymer chain may consist of over a thousand monomers, such that it is commonly assumed that the effect of crosslinks on the energy of mixing can be neglected. Moreover, following the approach by Flory [33], monomers of polymer chains and molecules of the two types of solvents are taken to be identical in size. Based on these assumptions, the free energy density of mixing W_{mix} for binary-solvent gels can be evaluated by exploiting the liquid lattice theory in which monomer solute is distributed in a solvent containing solvent molecules A and B (Fig. 2).

In the lattice model, we take unmixed polymer chains, pure solvent A, and pure solvent B as the reference state (Fig. 2(*a*)), and compare the energy change of the system before and after mixing the chains and solvents, i.e., the energy of the mixed system in Fig. 2(*b*) subtracts that of the reference state in Fig. 2(*a*). In this framework, the energy change, aka, the Helmholtz free energy of mixing F_{mix}, comprises two parts: the entropic contribution due to the alteration of configurational entropy and the enthalpic contribution arising from the heat of mixing. To determine the entropic contribution to F_{mix}, we estimate the number of ways of arranging N_A solvent molecules A, N_B solvent molecules B, and N_P polymer chains in a lattice consisting of $N = N_A + N_B + xN_P$ cells. Herein, x denotes the number of monomers in each polymer

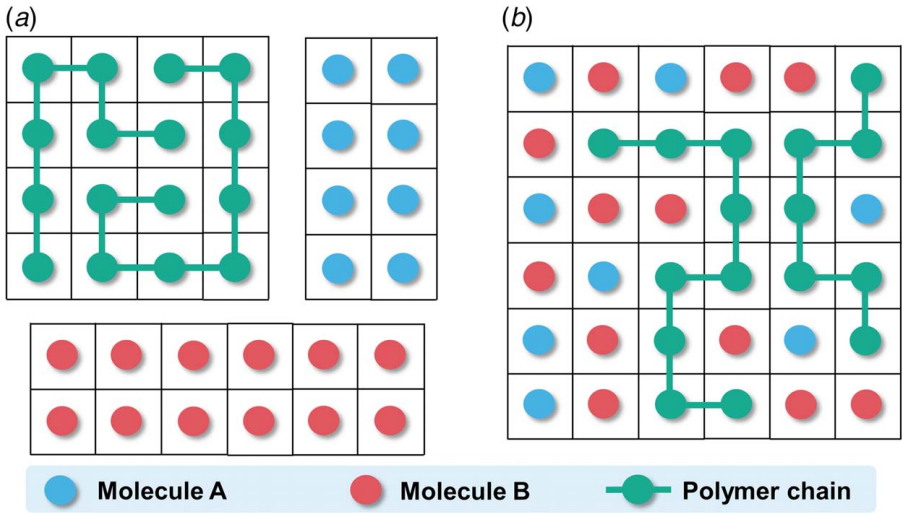

Fig. 2 A liquid lattice model in which polymer chains are distributed in a binary solvent comprising two types of solvent molecules (namely, molecules A and B). Each polymer chain consists of *x* monomers. It is assumed the monomers and the solvent molecules are identical in size. (*a*) The reference state of the system, that consists of unmixed polymer chains, pure solvent A, and pure solvent B. (*b*) The mixed state of the system.

chains; that is, each chain takes x contiguous sites in the lattice. The N_P polymer chains are consecutively added to the lattice, followed by the insertion of N_A molecules A and N_B molecules B. Suppose that i polymer chains have been randomly inserted into the lattice, the expected number of available arrangements for the chain $i+1$ can be approximated, with a trivial error, by

$$\Lambda_{i+1} = \left(\frac{Z-1}{N}\right)^{x-1} \frac{(N-xi)!}{[N-x(i+1)]!} \tag{3}$$

where Z represents the number of cells that are closest neighbors to a given cell and usually takes a value between 6 and 12 [33]. Therefore, the total number Ω_P of differentiable ways of arranging N_P polymer chains in the lattice comprising N cells is given by

$$\Omega_P = \frac{1}{N_P!}\prod_{0}^{N_P-1}\Lambda_{i+1} = \left(\frac{Z-1}{N}\right)^{N_P(x-1)} \frac{N!}{N_P!(N_A+N_B)!} \tag{4}$$

$N_A + N_B$ solvent molecules occupy the remaining lattice sites, and the number of possible arrangements, Ω_{AB}, can be evaluated by calculating the N_A combination of a (N_A+N_B)-set, such that

$$\Omega_{AB} = \binom{N_A+N_B}{N_A} = \frac{(N_A+N_B)!}{N_A!N_B!} \tag{5}$$

To this end, the product of Ω_P and Ω_{AB} gives the total number Ω of possible configurations for arranging N_P identical polymer chains, together with N_A solvent molecules A and N_B solvent molecules B, in the lattice consisting of $N = N_A + N_B + xN_P$ sites

$$\Omega = \Omega_P\Omega_{AB} = \left(\frac{Z-1}{N}\right)^{N_P(x-1)} \frac{N!}{N_P!N_A!N_B!} \tag{6}$$

It follows that according to the Boltzmann relation that the configurational entropy of the polymer solution should be given by $S_{\text{solution}} = k\ln\Omega$. Introduction of Stirling's approximation for factorials in Eq. (6) and subsequent simplifications yield

$$S_{\text{solution}} = -k\left[N_P\ln\frac{N_P}{N_A+N_B+xN_P} + N_A\ln\frac{N_A}{N_A+N_B+xN_P} + N_B\ln\frac{N_B}{N_A+N_B+xN_P} - N_P(x-1)\ln\frac{Z-1}{e}\right] \tag{7}$$

In the reference state (before mixing), the configurational entropy of the polymer chains can be evaluated by plugging Eq. (4) into $S_{\text{polymer}} = k\ln\Omega_P$ with $N_A = N_B = 0$, which gives

$$S_{\text{polymer}} = -k\left[-N_P\ln x - N_P(x-1)\ln\frac{Z-1}{e}\right] \tag{8}$$

Note that the configurational entropy of the pure solvent A, S_A, and that of pure solvent B, S_B, are both zero. We then subtract the configurational entropy of the reference state (i.e., $S_{\text{polymer}} + S_A + S_B$) from Eq. (7) to obtain the entropy of mixing polymer chains and the binary solvents

$$S_{\text{mix}} = S_{\text{solution}} - S_{\text{polymer}} - S_A - S_B = -k\left[N_P\ln\frac{xN_P}{N} + N_A\ln\frac{N_A}{N} + N_B\ln\frac{N_B}{N}\right] \tag{9}$$

Taking into account that the assumption pertaining to the lattice model, that is, the solute and solvent molecules are equal in volume, we recast Eq. (9) in the form

$$S_{\text{mix}} = -k[N_P\ln\phi_P + N_A\ln\phi_A + N_B\ln\phi_B] \tag{10}$$

where $\phi_P = xN_P/N$, $\phi_A = N_A/N$, and $\phi_B = N_B/N$ represent the volume fractions of polymer chains, solvents A and B, respectively.

The enthalpic part of F_{mix} stems from the energy change due to the formation of "contact pairs" between dissimilar molecules during mixing the pure components. By restrict our attentions to the interaction between nearest-neighbor molecules, the heat of mixing for the binary-solvent gel system is thus

$$H_{\text{mix}} = kT[\chi_{AP}N_A\phi_P + \chi_{BP}N_B\phi_P + \chi_{AB}N_B\phi_A] \tag{11}$$

where χ_{AP}, χ_{BP}, and χ_{AB} are dimensionless measures of the strength of pairwise interactions between molecules of different types, and for convenience, the lattice coordination number Z has been lumped into these dimensionless quantities [33].

By substituting Eqs. (10) and (11) into the definition of the Helmholtz free energy of mixing, i.e., $F_{\text{mix}} = H_{\text{mix}} - TS_{\text{mix}}$, we arrive at the expression for F_{mix}, that is,

$$F_{\text{mix}} = kT[N_P\ln\phi_P + N_A\ln\phi_A + N_B\ln\phi_B + \chi_{AP}N_A\phi_P + \chi_{BP}N_B\phi_P + \chi_{AB}N_B\phi_A] \tag{12}$$

One notes that it is important to choose the correct normalization volume for the free energy density of materials with changing volume. For convenience, we take the dry polymer network as the reference configuration, such that the free energy density W_{mix} is linked to the Helmholtz free energy of mixing F_{mix} in Eq. (12) by $W_{\text{mix}} = F_{\text{mix}}/(xN_P\nu)$, where ν is the volume of one monomer of the polymer chains. Hence, we have

$$W_{\text{mix}} = \frac{kT}{\nu}\left[\frac{1}{x}\ln\phi_P + \nu C_A\ln\phi_A + \nu C_B\ln\phi_B + \chi_{AP}\nu C_A\phi_P + \chi_{BP}\nu C_B\phi_P + \chi_{AB}\nu C_B\phi_A\right] \tag{13}$$

where $C_A = N_A/(xN_P\nu)$ and $C_B = N_B/(xN_P\nu)$ are nominal concentrations of solvent molecules in the gel, which are defined as the number of solvent molecules per unit volume of the dry polymer network. As noted above, x is the number of monomers in a polymer chain that commonly takes quite a large value in many gels. By setting $x\to\infty$, Eq. (13) reduces to

$$W_{\text{mix}} = \frac{kT}{\nu}[\nu C_A\ln\phi_A + \nu C_B\ln\phi_B + \chi_{AP}\nu C_A\phi_P + \chi_{BP}\nu C_B\phi_P + \chi_{AB}\nu C_B\phi_A] \tag{14}$$

Considering the assumption pertaining to the lattice model that the monomers and solvent molecules have the same volume ν, as well as the definition of C_A and C_B, it is straightforward to obtain the relations between ϕ_A, ϕ_B and C_A, C_B that

$$\phi_A = \frac{N_A}{N} = \frac{N_A\nu}{N_A\nu + N_B\nu + xN_P\nu} = \frac{C_A\nu}{C_A\nu + C_B\nu + 1} \tag{15a}$$

$$\phi_B = \frac{C_B\nu}{C_A\nu + C_B\nu + 1} \tag{15b}$$

$$\phi_P = 1 - \phi_A - \phi_B = \frac{1}{C_A\nu + C_B\nu + 1} \tag{15c}$$

Plugging Eqs. (2) and (14) into Eq. (1) yields the free energy density W of binary-solvent gels,

$$W = \frac{1}{2}NkT[F_{ik}F_{ik} - 3 - 2\log(\det\mathbf{F})] + \frac{kT}{\nu}[\nu C_A\ln\phi_A + \nu C_B\ln\phi_B + \chi_{AP}\nu C_A\phi_P + \chi_{BP}\nu C_B\phi_P + \chi_{AB}\nu C_B\phi_A] \tag{16}$$

The free energy density is defined using the dry state of the binary-solvent gel as the reference configuration. Note that setting $C_B = 0$ in Eq. (16) would reduce the above free energy function to that for single-solvent gels (e.g., hydrogels) which is given in Ref. [13].

2.2 The Equilibrium Equations. Figure 1 illustrates a gel in equilibrium with a binary-solvent environment and a set of mechanical forces and geometrical constraints. To be consistent with the free energy function given in Sec. 2.1 that is defined on the dry

state of the gel, we take the dry polymer network as the reference state in developing the equilibrium equations for the binary-solvent gel. $\mathbf{X}$ is the coordinate of a material element of the gel in the reference state. In the deformed state, the element moves to a place of the coordinate $\mathbf{x}$ so that the field $x_i(\mathbf{X})$ describes the deformation of the gel and the deformation gradient $\mathbf{F}$ is given by $F_{iK} = \partial x_i(\mathbf{X})/\partial X_K$. The field $C_A(\mathbf{X})$ and $C_B(\mathbf{X})$ describe the distribution of solvent molecules A and B in the gel. In Sec. 2.1, we took the three fields, $\mathbf{F}$, $C_A(\mathbf{X})$, and $C_B(\mathbf{X})$, as independent variables. However, the assumption of incompressibility of the gel imposes a constraint among these variables. Since the volume of the reference state (i.e., the dry polymer network) is $xN_p\nu$ based on the lattice model, the gel volume before and after swelling is correlated by $(xN_p\nu)\det\mathbf{F} = xN_p\nu + N_A\nu + N_B\nu$; dividing the equation by $xN_p\nu$ and considering the definition of C_A and C_B yield

$$1 + \nu C_A + \nu C_B = \det\mathbf{F} \tag{17}$$

Consequently, only two of the three variables vary independently and the third one is dictated by Eq. (17). In the present paper, we use the deformation gradient of the gel, $\mathbf{F}$, and the concentration of solvent molecule A, $C_A(\mathbf{X})$, as the two independent variables, such that the free energy function should be written as $W(\mathbf{F}, C_A)$.

A combination of Eqs. (15) and (17) gives that

$$\phi_A = \frac{\nu C_A}{\det\mathbf{F}} \tag{18a}$$

$$\phi_B = 1 - \frac{\nu C_A + 1}{\det\mathbf{F}} \tag{18b}$$

$$\phi_P = \frac{1}{\det\mathbf{F}} \tag{18c}$$

so that

$$W(\mathbf{F}, C_A) = \frac{1}{2}NkT[F_{iK}F_{iK} - 3 - 2\log J] + \frac{kT}{\nu}\left[\nu C_A \ln\frac{\nu C_A}{J} + (J - \nu C_A - 1)\ln\left(\frac{J - \nu C_A - 1}{J}\right) + \frac{\chi_{AP}\nu C_A}{J} + \frac{\chi_{BP}(J - \nu C_A - 1)}{J} + \frac{\chi_{AB}(J - \nu C_A - 1)\nu C_A}{J}\right] \tag{19}$$

where $J = \det\mathbf{F}$ denotes the volume ratio.

When the gel equilibrates with the external binary solvent and the mechanical forces, the change in the free energy of the binary-solvent gel is equal to the work done by applied mechanical forces and the external solvent

$$\int\delta W dV = \int B_i\delta x_i dV + \int T_i\delta x_i dA + \mu_A\int\delta C_A dV + \mu_B\int\delta C_B dV \tag{20}$$

where $B_i(\mathbf{X})$ and $T_i(\mathbf{X})$ are body forces and surface tractions applied on the gel and μ_A and μ_B represent the chemical potential of solvent molecule species A and B, respectively.

Equation (20) describes the thermodynamic equilibrium condition of a binary-solvent gel when the gel deforms by a small amount, $\delta x_i(\mathbf{X})$, and the solvent concentration changes by $\delta C_A(\mathbf{X})$ and $\delta C_B(\mathbf{X})$. The associated change in the free energy density is given by

$$\delta W(\mathbf{F}, C_A) = \frac{\partial W(\mathbf{F}, C_A)}{\partial F_{ik}}\delta F_{ik} + \frac{\partial W(\mathbf{F}, C_A)}{\partial C_A}\delta C_A \tag{21}$$

To apply the incompressibility condition (Eq. (17)) to the equilibrium equation (Eq. (20)), one notes that $\delta C_B(\mathbf{X})$ can be expressed in terms of a combination of $\delta x_i(\mathbf{X})$ and $\delta C_A(\mathbf{X})$ using the variational form of Eq. (17), that is

$$\delta C_B = \frac{1}{\nu}(\det\mathbf{F})H_{iK}\frac{\partial\delta x_i}{\partial X_K} - \delta C_A \tag{22}$$

where H_{iK} is the transpose of the inverse of the deformation gradient $\mathbf{F}$. By substituting Eqs. (21) and (22) into Eq. (20) and recognizing that the equation holds for any δx_i and δC_A, we reduce the equilibrium equation of the variational forms to that of the differential forms

$$\frac{\partial}{\partial X_k}\left[\frac{\partial W}{\partial F_{ik}} - \frac{\mu_B}{\nu}(\det\mathbf{F})H_{ik}\right] + B_i = 0 \tag{23a}$$

$$\frac{\partial \mathrm{W}}{\partial C_A} = \mu_A - \mu_B \tag{23b}$$

Equations (23a) and (23b) constitute equilibrium equations for binary-solvent gels. Equation (23a) is the force balance equation of the gel; therefore, the nominal stress s_{iK} is thus defined by

$$s_{iK} = \frac{\partial W}{\partial F_{ik}} - \frac{\mu_B}{\nu}(\det\mathbf{F})H_{ik} \tag{24}$$

Inserting the explicit form of the free energy function in Eq. (19) into Eqs. (23b) and (24) leads to

$$\frac{s_{iK}\nu}{kT} = N\nu(F_{iK} - H_{iK}) + \left[J\ln\left(1 - \frac{\nu C_A + 1}{J}\right) + 1 - \frac{\chi_{AP}\nu C_A}{J} + \frac{\chi_{BP}(\nu C_A + 1)}{J} + \frac{\chi_{AB}(\nu C_A + 1)\nu C_A}{J} - \frac{\mu_B}{kT}J\right]H_{iK} \tag{25a}$$

$$\frac{\mu_A}{kT} - \frac{\mu_B}{kT} = \ln\frac{\nu C_A}{J} + \frac{\chi_{AP}}{J} - \left[\ln\left(1 - \frac{\nu C_A + 1}{J}\right) + \frac{\chi_{BP}}{J}\right] + \chi_{AB}\left(1 - \frac{2\nu C_A + 1}{J}\right) \tag{25b}$$

In these equations of state, we have normalized the nominal stress by kT/ν and the chemical potential by kT. Note that combining Eqs. (25a) and (25b) to eliminate μ_B and setting $C_B = 0$ (i.e., $J = \nu C_A + 1$) would reduce the equations of state for binary-solvent gels to that for single-solvent gels (Eq. (18) in Ref. [13]), which in turn justifies the correctness of Eq. (25).

When the gel is in equilibrium with the external binary solvent, μ_A and μ_B are homogeneous in the gel and should equal to their external-solvent counterparts, namely,

$$\mu_A = \mu_A^s \tag{26a}$$

$$\mu_B = \mu_B^s \tag{26b}$$

According to the liquid lattice model presented above, the Helmholtz free energy of the external binary solvent is

$$F_s = kT\left[N_A^s\ln N_A^s + N_B^s\ln N_B^s - (N_A^s + N_B^s) \times \ln(N_A^s + N_B^s) + \chi_{AB}N_A^s\frac{N_B^S}{N_A^S + N_B^S}\right] \tag{27}$$

where N_A^s and N_B^s represent the number of molecules A and B in the external binary solvent. Therefore, the chemical potential of solvent molecules in the external binary solvent is

$$\frac{\mu_A^s}{kT} = \frac{\partial F_s}{\partial N_A^S} = \ln\phi_A^s + \chi_{AB}(1 - \phi_A^s)^2 \tag{28a}$$

$$\frac{\mu_B^s}{kT} = \frac{\partial F_s}{\partial N_B^S} = \ln\phi_B^s + \chi_{AB}(1 - \phi_B^s)^2 \tag{28b}$$

where $\phi_A^s = N_A^S/(N_A^S + N_B^S)$ and $\phi_B^s = 1 - \phi_A^s = N_B^S/(N_A^S + N_B^S)$ denote the volume fractions of molecules A and B in the external solvent, respectively, and are quantitative measures of the

composition of the external solvent. To this end, once ϕ_A^s is known, the composition of the binary solvent is characterized by ϕ_A^s and $\phi_B^s = 1 - \phi_A^s$, then Eq. (28) determine μ_A^s and μ_B^s. It follows that the deformation of the binary-solvent gel can be solved by inserting Eqs. (26) and (28) to Eq. (25). In the numerical examples to come in Sec. 3, we take the following values: $\chi_{AP} = \chi_{BP} = 0.2$, $\chi_{AB} = -0.9$, $N\nu = 10^{-3}$, and $kT = 4 \times 10^{-21}$ J for room temperature, unless otherwise mentioned. It is worthwhile to mention that we intentionally set $\chi_{AP} = \chi_{BP}$ in this study to show that the model has been developed correctly: for example, the free-swelling curve should be mirror-symmetrical given $\chi_{AP} = \chi_{BP}$ if the model is accurately formulated (see more details in Sec. 3.1). In real binary-solvent gels, each solvent may have different interplay characters with the polymer network. Different values of χ_{AP} and χ_{BP} can be readily adopted in the model to represent distinct behaviors of the two solvents (find examples in Sec. 3.5).

3 Results and Discussion

Hydrogels have been developed for diverse applications, including micro-valves [34], actuators [35], and sensors [36]. Many of these applications require hydrogels to swell and deform under external forces, or subject to mechanical constraints. In this section, the generic form of the constitutive model is fleshed out to examine the deformation of binary-solvent gels subject to different types of mechanical loadings and constraints.

3.1 Free Swelling of a Gel in a Binary Solvent. We first investigate the free-swelling behavior of binary-solvent gels in the absence of mechanical forces and constraints. When a dry polymer network is immersed in a binary solvent containing molecules A and B and is subject to no mechanical constraints and forces, the network could take in solvent molecules of both types and swell freely, resulting in a binary-solvent gel with an isotropic stretch ratio of $\lambda_1 = \lambda_2 = \lambda_3 = \lambda_0$. For this free-swelling process, Eqs. (25*a*) and (25*b*) reduce to

$$N\nu\left(\frac{1}{\lambda_0} - \frac{1}{\lambda_0^3}\right) + \ln\left(1 - \frac{\nu C_A + 1}{\lambda_0^3}\right) + \frac{1}{\lambda_0^3} - \frac{\chi_{AP}\nu C_A}{\lambda_0^6} + \frac{\chi_{BP}(\nu C_A + 1)}{\lambda_0^6} + \frac{\chi_{AB}(\nu C_A + 1)\nu C_A}{\lambda_0^6} = \frac{\mu_B^s}{kT} \tag{29a}$$

$$\frac{\mu_A^s}{kT} - \frac{\mu_B^s}{kT} = \ln\frac{\nu C_A}{\lambda_0^3} + \frac{\chi_{AP}}{\lambda_0^3} - \left[\ln\left(1 - \frac{\nu C_A + 1}{\lambda_0^3}\right) + \frac{\chi_{BP}}{\lambda_0^3}\right] + \chi_{AB}\left(1 - \frac{2\nu C_A + 1}{\lambda_0^3}\right) \tag{29b}$$

For a gel immersed in an external binary solvent with a given composition, the chemical potential μ_A^s and μ_B^s in Eq. (29) are specified by ϕ_A^s and ϕ_B^s through Eq. (28), such that the stretch ratio λ_0 and volume ratio of solvent A in the gel (relative to the dry polymer network), νC_A, can be solved from Eq. (29).

Figure 3(*a*) plots the total volume ratio of the gel, $J = \lambda_0^3$, as a function of ϕ_A^s, which measures the volume fraction of solvent A in the external binary solvent. As ϕ_A^s varies from 0 to 1, the binary-solvent gel first shrinks in size gradually, with the volume becoming minimum at $\phi_A^s = \phi_B^s = 0.5$, and then swells continuously until it recovers its original volume. As expected, the curve is mirror-symmetrical with the axis of symmetry being $\phi_A^s = 0.5$. The reason is that when χ_{AP} equals χ_{BP}, solvent molecule A and solvent molecule B are indifferentiable for the polymer network, such that, in terms of mechanical behavior, a gel equilibrating with an external solvent of $\phi_A^s = \phi$ and $\phi_B^s = 1 - \phi$ should be identical to that in equilibrium with a solvent of $\phi_A^s = 1 - \phi$ and $\phi_B^s = \phi$ (herein, $0 \le \phi \le 1$). Moreover, the abovementioned deswelling-to-swelling transition associated with increasing ϕ_A^s, which has been observed in many gels such as N-isopropylacrylamide (NIPAM) hydrogels in the alcohol-aqueous binary solvent [37], is recognized as the cononsolvency effect and is attributed to the negative value of $\chi_{AB} = -0.9$ adopted in the modeling. One notes that changing χ_{AB} from negative to positive would facilitate the transition from the cononsolvency effect to the cosolvency effect. The influence of χ_{AB} on the phenomena of cononcolvency and cosolvency has been systematically investigated by Xiao et al. [32]. In this paper, we will focus our attention on the mechanical behaviors of binary-solvent gels subjected to external forces and constraints but not elaborate on the effect of model parameters such as χ_{AB}. Also plotted in Fig. 3(*a*) are the volume ratio of solvent A (relative to the dry polymer network), νC_A, and that of solvent B, νC_B. With increasing ϕ_A^s in the external solvent, the content of solvent A in the gel continuously rises, whereas the content of solvent B diminishes. In a limiting case, namely, the gel is immersed in pure solvent A with $\phi_A^s = 1$, as expected, the volume ratio of solvent B becomes zero so that the gel is fully filled with solvent A. Likewise, the volume of solvent A vanishes when the gel is submerged in pure solvent B with $\phi_A^s = 0$.

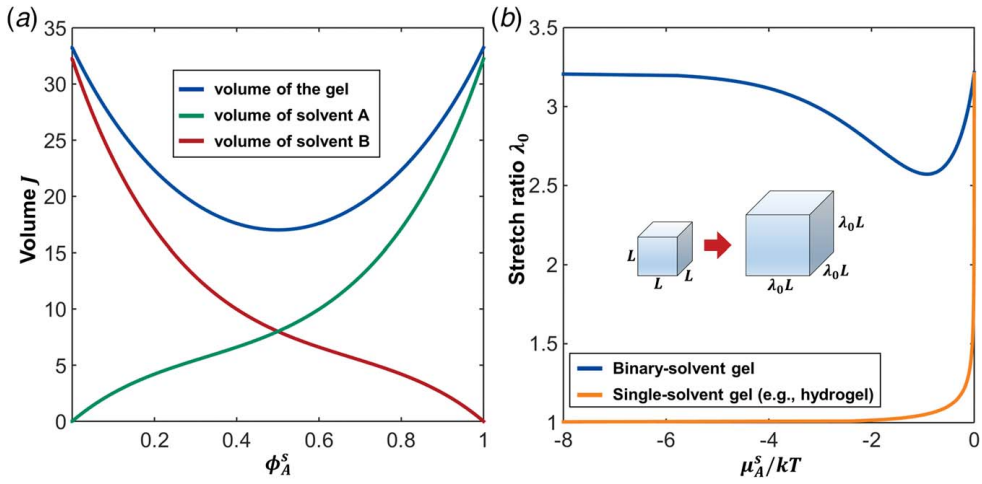

Fig. 3 (*a*) The volumes of free-swelling binary-solvent gels as a function of ϕ_A^s, the volume fraction of solvent A in the external solution. (*b*) The volumes of a binary-solvent gel and a single-solvent gel versus the chemical potential of solvent A in the external solvent.

To understand the free swelling of the binary-solvent gel better, in Fig. 3(*b*), we compare the free-swelling stretch λ_0 of binary-solvent gels, which contains both solvent molecules A and B, to that of single-solvent gels comprising solvent A only (e.g., hydrogels). Herein, a single-solvent gel refers to a polymer network that is permeable to only one type of solvent (named as solvent A in this case) in the external solution. The single-solvent gel is highly swollen when the chemical potential of solvent A, μ_A^s/kT, equals 0 in the external solution. As μ_A^s/kT decreases from 0, the single-solvent gel continuously expels the solvent, leading to a rapid reduction in the stretch ratio λ_0. When the chemical potential μ_A^s/kT drops below -2, the gel volume almost reduces to its dry-state volume because of exposing to extremely low amounts of solvent A in the external solution. These results are in line with the findings reported by Hong et al. [13]. By contrast, as μ_A^s/kT is varied from 0 (pure solvent A) to $-\infty$ (pure solvent B), the stretch of the binary-solvent gel declines first due to the outflow of solvent A and reaches a minimum at $\mu_A^s/kT = -0.92$ (corresponding to $\phi_A^s = 0.5$). Intriguingly, the size reduction is followed by a rebound in volume with λ_0 gradually increasing, since an increasing amount of solvent B migrates into the polymer network, offsetting the volume shrinking caused by the loss of solvent A.

3.2 A Gel Subject to Uniaxial Tension and in Equilibrium With a Binary Solvent. We next study the mechanical response of binary-solvent gels under mechanical forces. Consider a gel in equilibrium with a binary solvent comprising both solvents A and B, and subject to a uniaxial stress s_1. The deformation of the gel is characterized by the stretch λ_1 along the loading direction and two transverse stretches $\lambda_2 = \lambda_3$. According to Eq. (25), the applied nominal stress s_1 is related to the stretch λ_1 by

$$\frac{s_1\nu}{kT} = N\nu\left(\lambda_1 - \frac{1}{\lambda_1}\right) + \left[\lambda_2^2 \ln\left(1 - \frac{\nu C_A + 1}{\lambda_1\lambda_2^2}\right) + \frac{1}{\lambda_1} - \frac{\chi_{AP}\nu C_A}{\lambda_1^2\lambda_2^2} + \frac{\chi_{BP}(\nu C_A + 1)}{\lambda_1^2\lambda_2^2} + \frac{\chi_{AB}(\nu C_A + 1)\nu C_A}{\lambda_1^2\lambda_2^2} - \frac{\mu_B^s}{kT}\lambda_2^2\right] \tag{30a}$$

and the stresses in the transverse direction vanish, i.e.,

$$N\nu\left(\lambda_2 - \frac{1}{\lambda_2}\right) + \left[\lambda_1\lambda_2 \ln\left(1 - \frac{\nu C_A + 1}{\lambda_1\lambda_2^2}\right) + \frac{1}{\lambda_2} - \frac{\chi_{AP}\nu C_A}{\lambda_1\lambda_2^3} + \frac{\chi_{BP}(\nu C_A + 1)}{\lambda_1\lambda_2^3} + \frac{\chi_{AB}(\nu C_A + 1)\nu C_A}{\lambda_1\lambda_2^3} - \frac{\mu_B^s}{kT}\lambda_1\lambda_2\right] = 0 \tag{30b}$$

The chemical equilibrium is dictated by

$$\frac{\mu_A^s}{kT} - \frac{\mu_B^s}{kT} = \ln\frac{\nu C_A}{\lambda_1\lambda_2^2} + \frac{\chi_{AP}}{\lambda_1\lambda_2^2} - \left[\ln\left(1 - \frac{\nu C_A + 1}{\lambda_1\lambda_2^2}\right) + \frac{\chi_{BP}}{\lambda_1\lambda_2^2}\right] + \chi_{AB}\left(1 - \frac{2\nu C_A + 1}{\lambda_1\lambda_2^2}\right) \tag{30c}$$

These three equations together determine the stretches λ_1 and λ_2, and the volume of solvent A in the gel νC_A, given a applied stress s_1.

We plot the applied stress s_1 as a function of the stretch λ_1 in Fig. 4, with various values of ϕ_A^s. We find that, for gels immersed in the external solution with $0.5 \le \phi_A^s \le 1$, a larger ϕ_A^s leads to a more compliant response of the gel, namely, lower stress at the same stretch. The explanation is that the higher the value of ϕ_A^s, the more solvent the gel contains, and thus the more compliant the gel is. For this reason, the gel with $\phi_A^s = 0.5$ is stiffer than all others are since it holds the least amount of solvent as evidenced by Fig. 3(*a*). We also noticed that the stress–stretch curves of $\phi_A^s = 0.9$ and $\phi_A^s = 0.1$ coincide with each other because we take $\chi_{AP} = \chi_{BP}$ in the modeling and thus polymer chains cannot distinguish between solvent A and solvent B, such that polymer networks equilibrated with a solvent of $\phi_A^s = 0.9$ and $\phi_B^s = 0.1$ are identical to that in connection with a solvent of $\phi_A^s = 0.1$ and $\phi_B^s = 0.9$.

The stress-induced variation of the solvent content in gels is critical to the deformation and failure of structures made of gels [24,25,38]. For this, Figs. 4(*b*)–4(*d*) plot the total volumes of gels, as well as the volumes of solvents contained in the gels, as a function of the uniaxial stretch λ_1, with various values of ϕ_A^s. For gels immersed in a pure solvent A, i.e., $\phi_A^s = 1$, Fig. 4(*b*), the gel consecutively takes in solvent A as the stretch increases, causing simultaneous swelling and elongation of the gel. The prediction is in good agreement with results reported in the literature for hydrogels [24,38]. As expected, the gel does not hold any solvent B since it is connected to pure solvent A, such that the gel volume is the sum of the volume of the polymer network and that of the solvent A. In Fig. 4(*c*), it is demonstrated that the binary-solvent gel of $\phi_A^s = 0.9$ also expands in volume as it elongates, by taking in both solvent molecules of A and B from the external solution. Note that the external binary solution of $\phi_A^s = 0.9$ has 90% of solvent A in volume, hence the gel immersed in it also contains more solvent A than solvent B. Similarly, gels in contact with the binary solvent of $\phi_A^s = 0.5$ also swell in response to stretch and contain an equal amount of solvent A and solvent B, Fig. 4(*d*).

3.3 A Thin Layer of the Gel Bonded to a Rigid Substrate. This section examines how mechanical constraints affect the mechanical behaviors of binary-solvent gels. Specifically, we investigate the constrained swelling of a thin layer of the gel attached to a rigid substrate. The gel is initially fabricated in a binary solvent of ϕ_{A0}^s and then attached to the rigid substrate, where ϕ_{A0}^s denotes the initial volume fraction of solvent A in the external solvent. The associated pre-swelling stretch ratio is λ_0, which can be obtained by solving Eq. (29) with $\phi_A^s = \phi_{A0}^s$. When ϕ_A^s changes, the gel swells and deforms. We assume that the thickness of the gel is small compared to the dimensions in the plane of the substrate, such that the deformation of the gel is homogeneous. The two in-plane stretches are fixed to the pre-swelling stretch ratio λ_0 by the underlying substrate, and thus, the volume change of the gel is accommodated entirely by the expansion in the thickness direction with an out-of-plane stretch λ. In consequence, the gel develops an equibiaxial stress s in the plane of the substrate, the magnitude of which is given by

$$\frac{s\nu}{kT} = N\nu\left(\lambda_0 - \frac{1}{\lambda_0}\right) + \left[\lambda\lambda_0 \ln\left(1 - \frac{\nu C_A + 1}{\lambda\lambda_0^2}\right) + \frac{1}{\lambda_0} - \frac{\chi_{AP}\nu C_A}{\lambda\lambda_0^3} + \frac{\chi_{BP}(\nu C_A + 1)}{\lambda\lambda_0^3} + \frac{\chi_{AB}(\nu C_A + 1)\nu C_A}{\lambda\lambda_0^3} - \frac{\mu_B^s}{kT}\lambda\lambda_0\right] \tag{31a}$$

and the out-of-plane stress that is normal to the substrate vanishes, so that

$$0 = N\nu\left(\lambda - \frac{1}{\lambda}\right) + \left[\lambda_0^2 \ln\left(1 - \frac{\nu C_A + 1}{\lambda\lambda_0^2}\right) + \frac{1}{\lambda} - \frac{\chi_{AP}\nu C_A}{\lambda^2\lambda_0^2} + \frac{\chi_{BP}(\nu C_A + 1)}{\lambda^2\lambda_0^2} + \frac{\chi_{AB}(\nu C_A + 1)\nu C_A}{\lambda^2\lambda_0^2} - \frac{\mu_B^s}{kT}\lambda_0^2\right] \tag{31b}$$

Moreover, the chemical equilibrium equation can be obtained by setting the volume ratio $J = \lambda\lambda_0^2$ in Eq. (25*b*),

$$\frac{\mu_A^s}{kT} - \frac{\mu_B^s}{kT} = \ln\frac{\nu C_A}{\lambda\lambda_0^2} + \frac{\chi_{AP}}{\lambda\lambda_0^2} - \left[\ln\left(1 - \frac{\nu C_A + 1}{\lambda\lambda_0^2}\right) + \frac{\chi_{BP}}{\lambda\lambda_0^2}\right] + \chi_{AB}\left(1 - \frac{2\nu C_A + 1}{\lambda\lambda_0^2}\right) \tag{31c}$$

Equations (31*a*)–(31*c*) constitute the equations of state for constrained swelling of binary-solvent gels attached to a rigid substrate, from which λ, $s\nu/kT$, and νC_A can be solved given the initial state of the gel, namely, λ_0. We study the following numerical example: a binary-solvent gel is fabricated in an external solvent of $\phi_A^s = \phi_{A0}^s$,

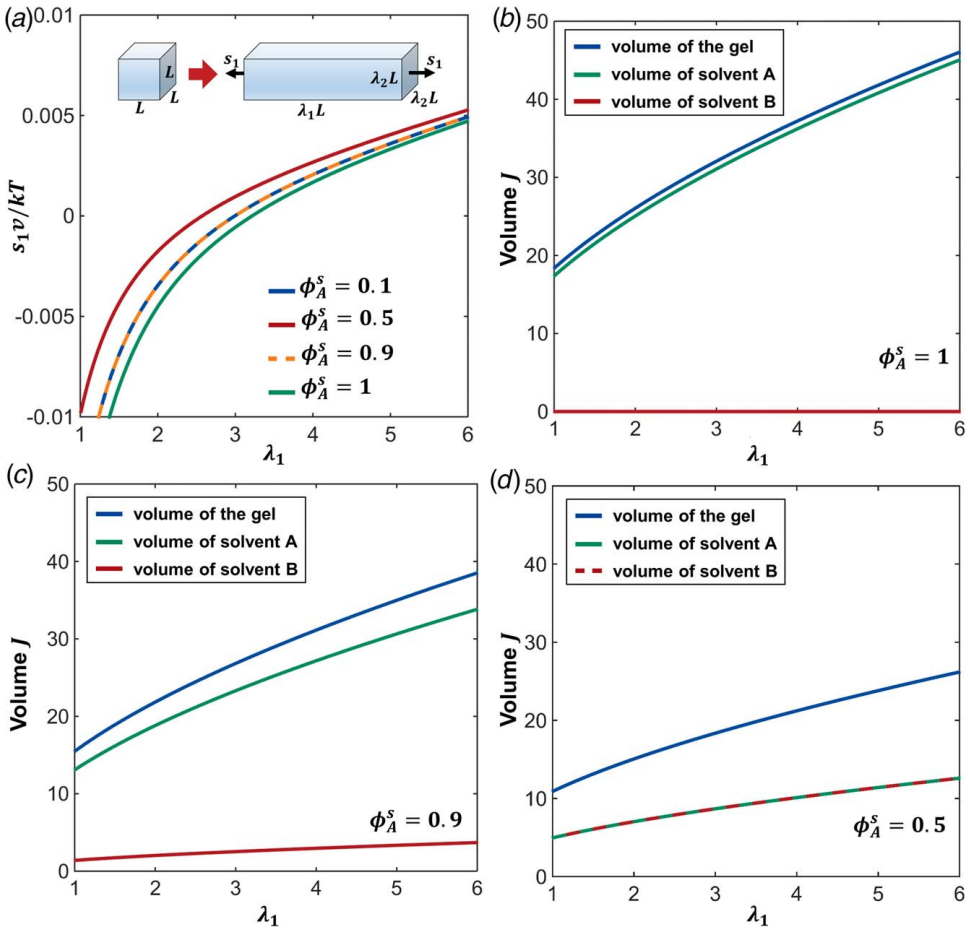

Fig. 4 A gel in equilibrium with a binary solvent is subject to a uniaxial stress. (*a*) The applied stress is plotted as a function of the stretch, with various values of ϕ_A^s. (*b*)–(*d*) The volumes of the gel, the solvent A, and the solvent B are plotted versus the stretch, for $\phi_A^s = 1$, 0.9, and 0.5, respectively.

thereafter the external solvent is added with more solvent A, which slowly increases ϕ_A^s from its original value to 1. Figures 5(*a*) and 5(*b*) plot the thickness ratio λ and in-plane stress s, respectively, as a function of ϕ_A^s for different values of ϕ_{A0}^s. It is shown that the thickness change is highly dependent on the pre-swelling state. For the gel fabricated in the solvent of $\phi_{A0}^s = 0.1$, as ϕ_A^s changes from 0.1 to 1, it becomes thinner first, reaching minimum thickness at $\phi_A^s = 0.5$, and then thickens gradually and eventually arrives at its largest thickness in pure solvent A of $\phi_A^s = 1$. The corresponding in-plane stress s rises at the beginning since the shrinking gel is stretched by the substrate to

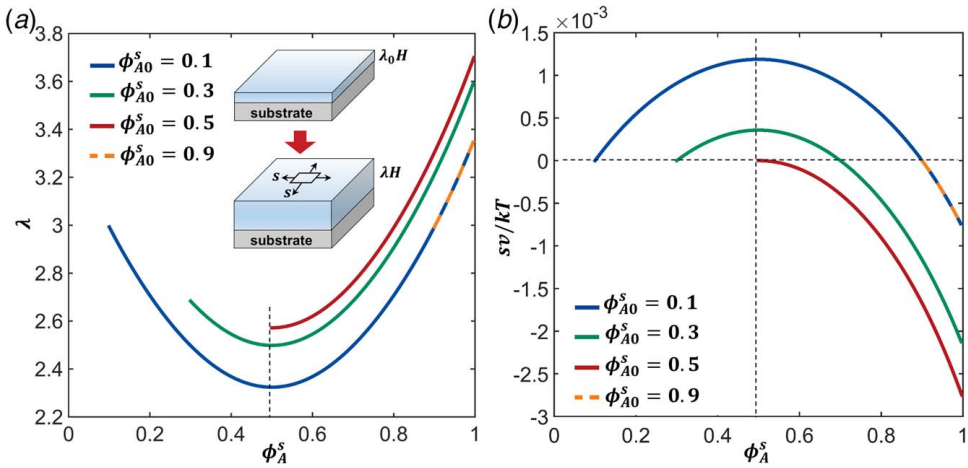

Fig. 5 A thin layer of the gel is bonded to a rigid substrate and in contact with a binary solvent of changing ϕ_A^s. (*a*) The gel changes its thickness in the direction normal to the layer to accommodate the volume change. The corresponding stretch ratio λ is plotted for gels with various initial conditions of ϕ_{A0}^s. (*b*) The gel develops an equal-biaxial stress s in the plane of the layer.

maintain the in-plane stretch λ_0. The initial increase in stress is followed by a decline once ϕ_A^s becomes larger than 0.5, which is attributed to the re-swelling of the gel. After ϕ_A^s exceeds 0.9, the gel expands beyond its initial volume so that it is squeezed in the plane of the substrate with a fixed in-plane stretch λ_0, rendering the stress s compressive. Similarly, the gel fabricated at $\phi_{A0}^s = 0.3$ also exhibits a thinning-to-thickening transition in thickness and a shift from tension to compression in in-plane stress, as ϕ_A^s changes from its original value 0.3 toward 1. In stark contrast, as is evident from Fig. 5(*a*), there exists no thinning stage for gels with initial conditions of $\phi_{A0}^s \geq 0.5$, since binary-solvent gels attain their minimal volume at $\phi_{A0}^s = 0.5$. Accordingly, these gels only undergo compression during the process, as shown in Fig. 5(*b*). Actuators and sensors are often designed by attaching a layer of the gel on the top of an elastic substrate, and the results presented here may shed light on novel designs based on binary-solvent gels.

Moreover, Fig. 5(*a*) demonstrates that gels subject to constrained swelling with distinct ϕ_{A0}^s attain different volumes at the same ϕ_A^s, while Fig. 3(*a*) shows that free-swelling gels should arrive at the same volume given a ϕ_A^s, regardless of their initial condition. The comparison indicates that mechanical constraints can markedly affect the volume of the gel.

3.4 A Bilayer Soft Actuator Based on Binary-Solvent Gels. Soft functional devices can be constructed by utilizing the swelling response of gels. Kuang et al. attached a cellulose hydrogel film to a passive polymer substrate, forming a cellulose-hydrogel-based bilayer soft actuator [39]. Since the cellulose-based hydrogel is prepared in an aqueous solution with relative humidity (RH) of 100%, exposing the bilayer actuator to the air environment of RH <100% expels water from the hydrogel, causing a significant decrease in the volume of the cellulose hydrogel film and thereby driving the bending of the bilayer to scroll up toward the gel side.

Binary-solvent gels can also be adopted to construct bilayer soft actuators. The inset of Fig. 6 illustrates the schematic of a bilayer actuator enabled by the binary-solvent gels. The gel fabricated in a binary solvent of ϕ_{A0}^s is attached to a passive substrate, and the pre-swelling stretch ratio λ_0 can be determined by solving Eq. (29). The as-made bilayer is flat with an initial curvature of $\kappa = 0$. When ϕ_A^s varies in the external binary solvents, the gel changes its volume and drives the bending of the bilayer actuators. By taking the gel layer as a thin film, the material state variables (strain, stress, and solvent concentration) remain the same through the film thickness, and the stress component normal to the gel surface vanishes, i.e., $s_3 = 0$. The stress component s_2 along the length direction of the film can be determined by analyzing the bending of the bilayer laminate, which yields,

$$s_2 = \frac{1 - \lambda_2/\lambda_0}{3} \frac{h_s}{h_f} E_s \tag{32}$$

where h_s and h_f denote the thickness of the substrate and the film, respectively and E_s represents Young's modulus of the substrate. Moreover, the contraction of the film along the width direction of the film is strongly restricted by the thick polymer substrate, such that $\lambda_1 = \lambda_0$ and the volume ratio $J = \lambda_0\lambda_2\lambda_3$. The governing equations for the bilayer soft actuator are comprised of three equations that

$$N\nu\left(\lambda_3 - \frac{1}{\lambda_3}\right) + \left[J\ln\left(1 - \frac{\nu C_A + 1}{J}\right) + 1 - \frac{\chi_{AP}\nu C_A}{J} + \frac{\chi_{BP}(\nu C_A + 1)}{J} + \frac{\chi_{AB}(\nu C_A + 1)\nu C_A}{J} - \frac{\mu_B^s}{kT}J\right]\frac{1}{\lambda_3} = 0 \tag{33a}$$

$$N\nu\left(\lambda_2 - \frac{1}{\lambda_2}\right) + \left[J\ln\left(1 - \frac{\nu C_A + 1}{J}\right) + 1 - \frac{\chi_{AP}\nu C_A}{J} + \frac{\chi_{BP}(\nu C_A + 1)}{J} + \frac{\chi_{AB}(\nu C_A + 1)\nu C_A}{J} - \frac{\mu_B^s}{kT}J\right]\frac{1}{\lambda_2} = \frac{1 - \lambda_2/\lambda_0}{3}\frac{h_s}{h_f}\frac{E_s\nu}{kT} \tag{33b}$$

$$\frac{\mu_A^s}{kT} - \frac{\mu_B^s}{kT} = \ln\frac{\nu C_A}{J} + \frac{\chi_{AP}}{J} - \left[\ln\left(1 - \frac{\nu C_A + 1}{J}\right) + \frac{\chi_{BP}}{J}\right] + \chi_{AB}\left(1 - \frac{2\nu C_A + 1}{J}\right) \tag{33c}$$

In the following calculations, the material properties being used are $E_s\nu/kT = 5N\nu$, $h_f/h_s = 0.1$, and $h_s = 1$ mm. Other parameters are taken as same as those used in previous calculations. We solve Eq. (33) for λ_2, λ_3, and νC_A at various ϕ_A^s. Then, the bending curvature can be evaluated by

$$\kappa = \frac{2(1 - \lambda_2/\lambda_0)}{h_s} \tag{34}$$

In Fig. 6, the bending curvature κ, a measurement of the actuation performance, is plotted as a function of ϕ_A^s ($0.5 \leq \phi_A^s \leq 1$), for various values of ϕ_{A0}^s. It can be seen that the bilayer actuator remains flat for $\phi_A^s = \phi_{A0}^s$. For $\phi_A^s < \phi_{A0}^s$, the gel film loses solvents and shrinks in volume, driving the bilayer to bend toward the gel side and rendering the curvature κ positive. On the contrary, for $\phi_A^s > \phi_{A0}^s$, the absorption of solvents leads to the volume expansion of the gel film, and thus, the laminate rolls up toward the substrate side, causing a negative curvature.

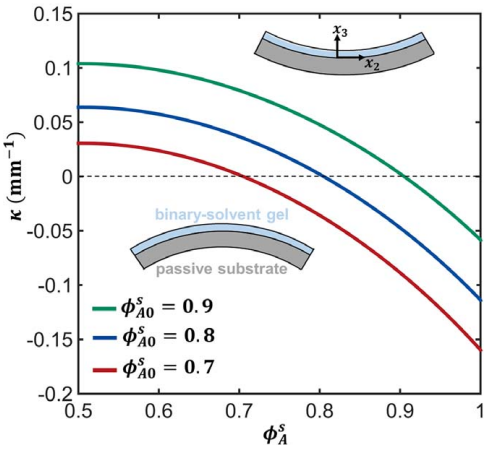

Fig. 6 Bending curvature of the bilayer soft actuator as a function of the volume fraction of solvent A in the external binary solvents. The inset shows the schematic of the bilayer actuator consisting of a binary-solvent gel film attached to a passive polymer substrate.

3.5 Comparison With Experimental Results. In this section, to verify the model developed in this work, we will apply the model to characterize experimental results recently reported in Ref. [40]. As a brief description of the experiment, random copolymer gels of NIPAM and N-ethylacrylamide were synthesized. The free-swelling behavior of the gels was studied by immersing the gels in different methanol–water mixtures, and the swelling ratio was recorded as a function of the volume fraction of methanol in the methanol–water binary solvents. It was revealed the swelling ratio minimizes at a volume fraction of methanol around $\phi_{\text{methanol}}^s = 0.35$, which is known as the cononsolvency effect. In this study, we use Eq. (29) to characterize the free swelling of gels in the methanol–water binary solvents. The dimensionless modulus of the gel is taken to be $N\nu = 10^{-3}$. Other model parameters are determined by fitting Eq. (29) to the experimental data, and we find $\chi_{AP} = 0.28$, $\chi_{BP} = 0.2$, and $\chi_{AB} = -0.95$. Note that solvent A

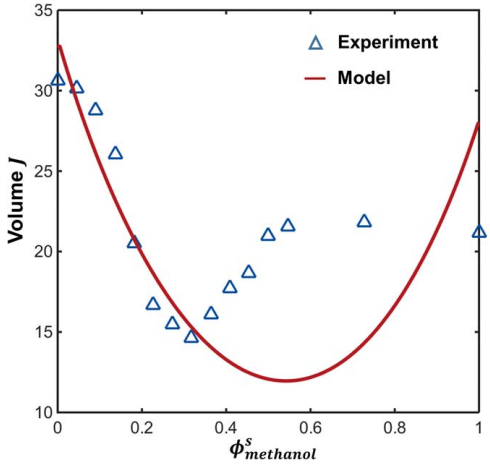

Fig. 7 Comparison of the model's prediction with experimental data for gels immersed in methanol–water binary solvents. The experimental data are extracted from Ref. [40].

represents methanol and solvent B is water in this case. As shown in Fig. 7, the theoretically fitted curve matches reasonably well with experimental results, indicating that our model can well capture the intricate interplays among polymer chains, methanol, and water. We would like to emphasize that the discrepancy between the model's predictions and experimental results is mainly attributed to the simple Flory–Huggins lattice theory used here. Adopting an alternative form of W_{mix} may better fit the experimental results but is not the objective of this paper. Moreover, experimental data on binary-solvent gels under mechanical loads are still lacking, we thus call for further experimental studies to demonstrate the research findings from the present study.

4 Conclusions

In this study, we developed a constitutive model for binary-solvent gels, which refer to gels comprising two types of solvent molecules (e.g., gels in aqueous alcohols) [10,11], and studied their mechanical responses to mechanical loadings and geometric constraints. We first formulated the free energy function for binary-solvent gels by extending the Flory–Huggins lattice model and derived the equilibrium equations in generic forms. Since applications of gels often require them to swell and deform under constraints or external forces. The theoretical model was then applied to examine various types of deformation modes of binary-solvent gels, including free swelling, uniaxial tension, and constrained swelling. Our modeling successfully captured some experimental findings about binary-solvent gels such as the cononsolvency effect. Moreover, we analyzed the actuation of a bilayer soft actuator that consists of binary-solvent gels attaching to a polymer substrate. We expect the proposed model to deliver insights into the deformation mechanics of binary-solvent gels and promote the development of this novel type of the soft material toward soft machines with enhanced functional applications.

Funding Data

- National Natural Science Foundation of China (Grant No. 11802269).

References

[1] Liu, M., Zeng, X., Ma, C., Yi, H., Ali, Z., Mou, X., Li, S., Deng, Y., and He, N., 2017, "Injectable Hydrogels for Cartilage and Bone Tissue Engineering," Bone Res., **5**(1), p. 17014.

[2] Prince, E., and Kumacheva, E., 2019, "Design and Applications of Man-Made Biomimetic Fibrillar Hydrogels," Nat. Rev. Mater., **4**(2), pp. 99–115.

[3] Li, J., and Mooney, D. J., 2016, "Designing Hydrogels for Controlled Drug Delivery," Nat. Rev. Mater., **1**(12), p. 16071.

[4] Han, Z., Wang, P., Mao, G., Yin, T., Zhong, D., Yiming, B., Hu, X., Jia, Z., Nian, G., Qu, S., and Yang, W., 2020, "A Dual pH-Responsive Hydrogel Actuator for Lipophilic Drug Delivery," ACS Appl. Mater. Interfaces., **12**(10), pp. 12010–12017.

[5] Ashley, G. W., Henise, J., Reid, R., and Santi, D. V., 2013, "Hydrogel Drug Delivery System With Predictable and Tunable Drug Release and Degradation Rates," Proc. Natl. Acad. Sci. USA, **110**(6), pp. 2318–2323.

[6] Yuk, H., Lu, B., and Zhao, X., 2019, "Hydrogel Bioelectronics," Chem. Soc. Rev., **48**(6), pp. 1642–1667.

[7] Lu, B., Yuk, H., Lin, S., Jian, N., Qu, K., Xu, J., and Zhao, X., 2019, "Pure PEDOT:PSS Hydrogels," Nat. Commun., **10**, p. 1043.

[8] Shi, Y., Peng, L., and Yu, G., 2015, "Nanostructured Conducting Polymer Hydrogels for Energy Storage Applications," Nanoscale, **7**(30), pp. 12796–12806.

[9] Yin, T., Wu, L., Wu, T., Mao, G., Nian, G., Chen, Z., Hu, X., Wang, P., Xiang, Y., Yu, H., Qu, S., and Yang, W., 2019, "Ultrastretchable and Conductive Core/Sheath Hydrogel Fibers With Multifunctionality," J. Polym. Sci. Part B—Polym. Phys., **57**(5), pp. 272–280.

[10] Lou, Y., Wang, Y., Li, Y., He, M., Su, N., Xu, R., Meng, X., Hou, B., and Xie, C., 2018, "Thermodynamic Equilibrium and Cosolvency of Florfenicol in Binary Solvent System," J. Mol. Liq., **251**, pp. 83–91.

[11] Kong, L., Zhang, F., Xing, P., Chu, X., and Hao, A., 2017, "A Binary Solvent Gel as Drug Delivery Carrier," Colloids Surf. A—Physicochem. Eng. Aspects, **522**, pp. 577–584.

[12] Han, L., Liu, K., Wang, M., Wang, K., Fang, L., Chen, H., Zhou, J., and Lu, X., 2018, "Mussel-Inspired Adhesive and Conductive Hydrogel With Long-Lasting Moisture and Extreme Temperature Tolerance," Adv. Funct. Mater., **28**(3), p. 1704195.

[13] Hong, W., Liu, Z., and Suo, Z., 2009, "Inhomogeneous Swelling of a Gel in Equilibrium With a Solvent and Mechanical Load," Int. J. Solids Struct., **46**(17), pp. 3282–3289.

[14] Cai, S., and Suo, Z., 2011, "Mechanics and Chemical Thermodynamics of Phase Transition in Temperature-Sensitive Hydrogels," J. Mech. Phys. Solids, **59**(11), pp. 2259–2278.

[15] Yu, Y., Landis, C. M., and Huang, R., 2017, "Salt-Induced Swelling and Volume Phase Transition of Polyelectrolyte Gels," ASME J. Appl. Mech., **84**(5), p. 051005.

[16] Marcombe, R., Cai, S., Hong, W., Zhao, X., Lapusta, Y., and Suo, Z., 2010, "A Theory of Constrained Swelling of a pH-Sensitive Hydrogel," Soft Matter, **6**(4), p. 784.

[17] Dehghany, M., Zhang, H., Naghdabadi, R., and Hu, Y., 2018, "A Thermodynamically-Consistent Large Deformation Theory Coupling Photochemical Reaction and Electrochemistry for Light-Responsive Gels," J. Mech. Phys. Solids, **116**, pp. 239–266.

[18] Xuan, C., and Jin, L., 2019, "Concurrent Reaction and Diffusion in Photo-Responsive Hydrogels," J. Mech. Phys. Solids, **124**, pp. 599–611.

[19] Zheng, Y., Hu, Y., and Cai, S., 2019, "Contact Mechanics of a Gel Under Constrained Swelling," J. Mech. Phys. Solids, **124**, pp. 427–445.

[20] Wang, Q., and Gao, Z., 2016, "A Constitutive Model of Nanocomposite Hydrogels With Nanoparticle Crosslinkers," J. Mech. Phys. Solids, **94**, pp. 127–147.

[21] Lu, T., Wang, Z., Tang, J., Zhang, W., and Wang, T., 2020, "A Pseudo-Elasticity Theory to Model the Strain-Softening Behavior of Tough Hydrogels," J. Mech. Phys. Solids, **137**, p. 103832.

[22] An, Y., Solis, F. J., and Jiang, H., 2010, "A Thermodynamic Model of Physical Gels," J. Mech. Phys. Solids, **58**(12), pp. 2083–2099.

[23] Chester, S. A., 2012, "A Constitutive Model for Coupled Fluid Permeation and Large Viscoelastic Deformation in Polymeric Gels," Soft Matter, **8**(31), p. 8223.

[24] Cheng, J., Jia, Z., Guo, H., Nie, Z., and Li, T., 2019, "Delayed Burst of a Gel Balloon," J. Mech. Phys. Solids, **124**, pp. 143–158.

[25] Wang, H., and Cai, S., 2015, "Drying-Induced Cavitation in a Constrained Hydrogel," Soft Matter, **11**(6), pp. 1058–1061.

[26] Fu, Y., Lu, H., Nian, G., Wang, P., Lin, N., Hu, X., Zhou, H., Yu, H., Qu, S., and Yang, W., 2020, "Size-Dependent Inertial Cavitation of Soft Materials," J. Mech. Phys. Solids, **137**, p. 103859.

[27] Wang, Q., Gao, Z., and Yu, K., 2017, "Interfacial Self-Healing of Nanocomposite Hydrogels: Theory and Experiment," J. Mech. Phys. Solids, **109**, pp. 288–306.

[28] Long, R., Mayumi, K., Creton, C., Narita, T., and Hui, C. Y., 2014, "Time Dependent Behavior of a Dual Cross-Link Self-Healing Gel: Theory and Experiments," Macromolecules, **47**(20), pp. 7243–7250.

[29] Zhou, Y., Hu, J., and Liu, Z., 2019, "Deformation Behavior of Fiber-Reinforced Hydrogel Structures," Int. J. Struct. Stab. Dyn., **19**(3), p. 1950032.

[30] Yang, T. H., and Lue, S. J., 2012, "Modeling Sorption Behavior for Ethanol/Water Mixtures in a Cross-Linked Polydimethylsiloxane Membrane Using the Flory–Huggins Equation," J. Macromol. Sci. Part B, **52**(7), pp. 1009–1029.

[31] Arndt, M. C., and Sadowski, G., 2012, "Modeling Poly(N-Isopropylacrylamide) Hydrogels in Water/Alcohol Mixtures With PC-SAFT," Macromolecules, **45**(16), pp. 6686–6696.

[32] Xiao, R., Qian, J., and Qu, S., 2019, "Modeling Gel Swelling in Binary Solvents: A Thermodynamic Approach to Explaining Cosolvency and Cononsolvency Effects," Int. J. Appl. Mech., **11**(05), p. 1950050.

[33] Flory, P. J., 1953, *Principles of Polymer Chemistry*, Cornell University Press, Ithaca.

[34] Song, J. E., and Cho, E. C., 2016, "Dual-Responsive and Multi-Functional Plasmonic Hydrogel Valves and Biomimetic Architectures Formed With Hydrogel and Gold Nanocolloids," Sci. Rep., **6**, p. 34622.

[35] Yuk, H., Lin, S., Ma, C., Takaffoli, M., Fang, N. X., and Zhao, X., 2017, "Hydraulic Hydrogel Actuators and Robots Optically and Sonically Camouflaged in Water," Nat. Commun., **8**, p. 14230.
[36] Lee, W., Kalashnikov, N., Mok, S., Halaoui, R., Kuzmin, E., Putnam, A. J., Takayama, S., Park, M., McCaffrey, L., Zhao, R., Leask, R. L., and Moraes, C., 2019, "Dispersible Hydrogel Force Sensors Reveal Patterns of Solid Mechanical Stress in Multicellular Spheroid Cultures," Nat. Commun., **10**, p. 144.
[37] Huther, A., Xu, X. P., and Maurer, G., 2004, "Swelling of n-Isopropyl Acrylamide Hydrogels in Water and Aqueous Solutions of Ethanol and Acetone," Fluid Phase Equilib., **219**(2), pp. 231–244.
[38] Wang, X., and Hong, W., 2012, "Delayed Fracture in Gels," Soft Matter, **8**(31), pp. 8171–8178.
[39] Kuang, Y., Chen, C., Cheng, J., Pastel, G., Li, T., Song, J., Jiang, F., Li, Y., Zhang, Y., Jang, S. H., Chen, G., Li, T., and Hu, L., 2019, "Selectively Aligned Cellulose Nanofibers Towards High-Performance Soft Actuators," Extreme Mech. Lett., **29**, p. 100463.
[40] Biswas, C. S., Wang, Q., Du, B., and Stadler, F. J., 2017, "Testing of the Effect of Parameters on the Cononsolvency of Random Copolymer Gels of N-Isopropylacrylamide and N-Ethylacrylamide in Methanol-Water Mixed Solvents by Simple Gravimetric Method," Polym. Test., **62**, pp. 177–188.